Patrick D. Lomenzo, Stefan Slesazeck, Michael Hoffmann, Thomas Mikolajick, Uwe Schroeder, Benjamin Max

# Ferroelectric Hf1-xZrxO2 memories: device reliability and depolarization fields

**Erstveröffentlichung in / First published in:**

*2019 19th Non-Volatile Memory Technology Symposium (NVMTS)*. Durham, 28.-30. Oktober 2019. IEEE. ISBN 978-1-7281-4431-3

DOI: https://doi.org/10.1109/NVMTS47818.2019.9043368

Final edited form was published in " 2019 19th Non-Volatile Memory Technology Symposium (NVMTS). Durham, 2019." ISBN 978-1-7281-4431-3
https://doi.org/10.1109/NVMTS47818.2019.9043368

# Ferroelectric $Hf_{1-x}Zr_xO_2$ Memories: Device Reliability and Depolarization Fields

Patrick D. Lomenzo, Stefan Slesazeck, Michael Hoffmann, Thomas Mikolajick, Uwe Schroeder
NaMLab gGmbH
Dresden, Germany
patrick.lomenzo@namlab.com

Benjamin Max, Thomas Mikolajick
Chair of Nanoelectronic Materials
TU Dresden
Dresden, Germany
thomas.mikolajick@tu-dresden.de

**The influence of depolarization and its role in causing data retention failure in ferroelectric memories is investigated. Ferroelectric $Hf_{0.5}Zr_{0.5}O_2$ thin films 8 nm thick incorporated into a metal-ferroelectric-metal capacitor are fabricated and characterized with varying thicknesses of an $Al_2O_3$ interfacial layer. The magnitude of the depolarization field is adjusted by controlling the thickness of the $Al_2O_3$ layer. The initial polarization and the change in polarization with electric field cycling is strongly impacted by the insertion of $Al_2O_3$ within the device stack. Transient polarization loss is shown to get worse with larger depolarization fields and data retention is evaluated up to 85 °C.**

***Ferroelectrics; FRAM; Depolarization; Retention; Wake-up; Memory Reliability***

## I. Introduction

The fast and low-power read/write (RW) operation of ferroelectric memories make them an intriguing class of alternative non-volatile memory technologies. Since ferroelectricity has been shown to emerge in thin (< 10nm) $HfO_2$-$ZrO_2$ films [1], [2], higher density ferroelectric memories have become a tangible possibility. Such ferroelectric memories include (anti)ferroelectric random access memory (A)FeRAM [3], [4] and ferroelectric tunnel junctions (FTJs) [5] based on capacitor device structures, as well as ferroelectric field effect transistors (FeFETs) which employ the ferroelectric in the gate-stack of a transistor [6]. A fundamental understanding of the reliability characteristics influencing ferroelectric $Hf_xZr_{1-x}O_2$ (HZO) devices remains a key challenge for demonstrating robust, long-term data retention and reliable operation.

Due to the polar nature of ferroelectrics, the generation of a depolarization field is inevitable, strongly influencing the characteristics of thin films [7]. By taking into account the finite screening length of charge carriers at the electrode interfaces or by inserting an interfacial dielectric layer in between the ferroelectric and the metal electrodes, the depolarization field can be evaluated. The strength of the depolarization field is considered to be a primary reason for long-term data retention failure in FeFETs [8]. Depolarization is likely to be a significant concern for two layer ferroelectric tunnel junctions [9] and to a lesser extent conventional FRAM. It is therefore of great interest to learn more about how the depolarization field can be implicated in several aspects of ferroelectric $Hf_xZr_{1-x}O_2$ performance including: (1) wake-up cycling, (2) transient polarization loss, and (3) long term data retention.

Ferroelectric thin films have been observed to undergo an improvement in remanent polarization with electric field cycling often referred to as wake-up [10], [11]. The principle causes of wake-up are thought to arise from domain depinning and/or a phase transition due to the field driven migration and redistribution of defects [11], [12]. It is unclear what the impact of the depolarization field is on wake-up cycling or to what extent depolarization suppresses the initial remanent polarization. Since wake-up is seen in both FeRAM and FeFET devices [13], [14], a better understanding of the phenomena is needed for device reliability modeling. Moreover, both short term transient polarization loss and long-term data retention can be evaluated by carefully adjusting the depolarization field and thus aid in predicting long term data retention characteristics of FeFETs,

To evaluate the implications the depolarization field has on the reliability characteristics of ferroelectric hafnium-oxide based non-volatile memory devices, the paper is split into the following sections: First, the finite screening length and interfacial dead layer depolarization models are introduced. Following the depolarization models, device fabrication and electrical measurements are then detailed. The device reliability performance brings the paper to its conclusion on the important consequences of depolarization in ferroelectric non-volatile memories.

## II. Depolarization Mechanisms

### A. Finite Screening Length in Metal Electrodes

When a ferroelectric is polarized by an external electric field, the surface charges produced by the ferroelectric dipoles lead to a corresponding free carrier redistribution within the terminating electrodes at the ferroelectric interfaces. The redistributed charge carriers within the electrode at the interface are screening charges which stabilize the ferroelectric dipoles and reduce the depolarization field. Nonetheless, ideal screening can only occur when the sheet of compensating charge has zero thickness. In practice, metals (and to a greater extent semiconductors) exhibit screening charge which extends a certain depth away from the ferroelectric interface which is called the screening length. The screening length is defined as

Final edited form was published in " 2019 19th Non-Volatile Memory Technology Symposium (NVMTS). Durham, 2019." ISBN 978-1-7281-4431-3
https://doi.org/10.1109/NVMTS47818.2019.9043368

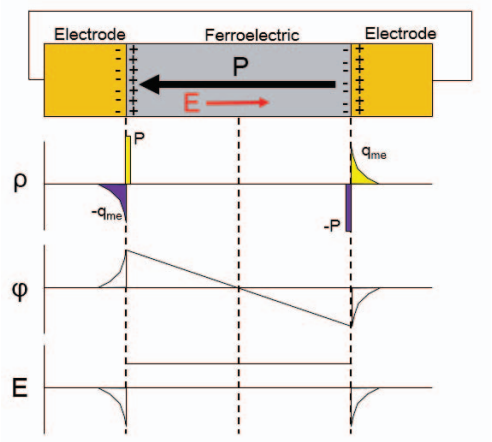


Figure 1. A ferroelectric film in a polarized state with compensating screening charges at the metal electrode interfaces. The charge density, potential, and electric field profiles are shown in descending order (not drawn to scale).

$$l_s=\left(\frac{h}{q}\right)\sqrt{\frac{\varepsilon_0\varepsilon_m}{3m_*}}\left(\frac{3}{8\pi}\right)^{1/3}\left(\frac{1}{n_0}\right)^{1/6} \quad (1)$$

where h is the Planck constant, q the elementary unit of charge, $n_0$ the equilibrium electron density in the metal, $m_*$ the effective electron mass, $\varepsilon_0$ the free space permittivity, and $\varepsilon_m$ the relative permittivity of the metal.

Finite screening is illustrated in Fig. 1 where the charge distribution within the metal exhibits a spatial extent defined by the screening length and the ferroelectric material is assumed to be perfectly insulating. By solving Poisson's equation [7], one can calculate the surface screening charge at both metal-ferroelectric interfaces as

$$q_{me}=\mp P\frac{\left(\frac{d_{FE}}{2\varepsilon_{FE}}\right)}{\left(\frac{d_{FE}}{2\varepsilon_{FE}}\right)+\left(\frac{l_s}{\varepsilon_m}\right)} \quad (2)$$

where P is the ferroelectric polarization surface charge, $d_{FE}$ is the ferroelectric thickness, $\varepsilon_{FE}$ and $\varepsilon_m$ is the relative permittivity of the ferroelectric and metal respectively. Note that P in (2) is surface charge and not the polarization vector. The electric field or depolarization field which arises from the imperfect screening of the ferroelectric dipoles can then be expressed as

$$E_{FE}=\frac{q_{me}\pm P}{\varepsilon_0\varepsilon_{FE}}. \quad (3)$$

It can be seen that if the finite screening length is zero in (2), the depolarization field disappears in (3). At the other extreme, if the screening length approaches infinity, an extremely large depolarization field is produced by the ferroelectric polarization. Such strong fields could make the ferroelectric polarization inherently unstable and lead to randomized domain formation to reduce the free energy in the ferroelectric. One can see from (2) that the screening charge density at the interface is further diminished as the ferroelectric thickness is decreased.

### *B. Interfacial Dielectric Layer*

It is widely reported that ferroelectrics exhibit a non-switching or 'dead' interfacial dielectric layer which degrades the ferroelectric properties as the film thickness is scaled down [15], [16]. Like the case of finite screening in metal electrodes, a depolarization field is generated as a result of a dielectric layer in series with the ferroelectric capacitor as seen in Fig. 2. In the symmetrical case where both interfacial layers are of thickness $d_{int}/2$ and have the same relative permittivity, one can express the resulting equivalent capacitance as

$$C_T=\frac{C_{FE}C_{int}}{C_{FE}+C_{int}}=\frac{\varepsilon_0\varepsilon_{FE}\varepsilon_{int}}{\varepsilon_{FE}d_{int}+\varepsilon_{int}d_{FE}} \quad (4)$$

where $C_{FE}$ is the capacitance of the ferroelectric, $C_{int}$ is the interfacial capacitance, and $\varepsilon_{int}$ is the relative permittivity of the interfacial layer.

To solve the electrostatic boundary conditions and determine the depolarization field, we first consider the voltage expressed as

$$V=d_{FE}E_{FE}+d_{int}E_{int} \quad (5)$$

where $E_{int}$ is defined as the electric field across the interfacial layer. The displacement field of the ferroelectric and the dielectric interfacial layer are then considered respectively:

$$D_{FE}=\varepsilon_0\varepsilon_{FE}E_{FE}+P \quad (6)$$

$$D_{int}=\varepsilon_0\varepsilon_{int}E_{int}. \quad (7)$$

Considering short circuit conditions where V = 0 and $D_{int}$=$D_{FE}$, (5) – (7) yields the depolarization field as

$$E_{FE}=\frac{-Pd_{int}}{\varepsilon_0\left(d_{int}\varepsilon_{FE}+d_{FE}\varepsilon_{int}\right)}. \quad (8)$$

The two properties of the interfacial layer which are impacting the depolarization field in (8) are the relative permittivity, a material property, and the thickness which can be changed during deposition. Thicker interfacial layers and lower dielectric constant interface layers serve to strengthen the depolarization field. With regard to the ferroelectric, since the relative permittivity is generally fixed, thinner films also heighten the magnitude of the depolarization field. Due to the displacement field boundary conditions and neglecting any free charge at the dielectric/ferroelectric interface, the field across the interfacial layer is

Final edited form was published in " 2019 19th Non-Volatile Memory Technology Symposium (NVMTS). Durham, 2019." ISBN 978-1-7281-4431-3
https://doi.org/10.1109/NVMTS47818.2019.9043368

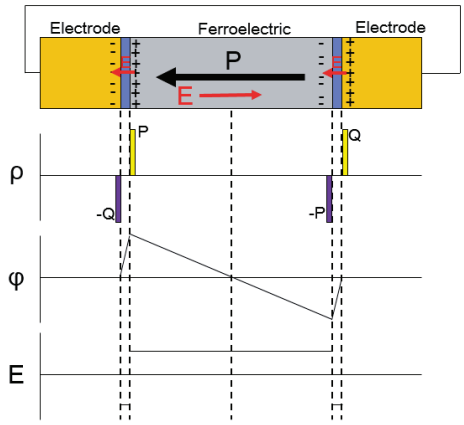


Figure 2. Nonferroelectric dielectric interfacial layers produce similar charge density, potential, and electric field distributions as finite screening in metal electrodes (not drawn to scale).

$$E_{int} = \frac{Pd_{FE}}{\varepsilon_0(d_{int}\varepsilon_{FE} + d_{FE}\varepsilon_{int})}. \qquad (9)$$

The field across the interfacial layer can be very large when $d_{FE}/d_{int} > 1$ and $\varepsilon_{FE}/\varepsilon_{int} > 1$ such that charge carriers can be injected between the interfacial layer and the ferroelectric. Charge injection across the dead interfacial layer has been predicted to be the cause of imprint or voltage shifts, where one polarization state is stabilized at the expense of the opposite polarization state [17], [18]. If one considers charge injection between the dielectric and ferroelectric, the interfacial dead layer model shares further similarities to the finite screening case due to screening charge. Thus, in the interfacial dead layer model both depolarization and imprint phenomena can be modeled to more accurately predict long-term data retention in ferroelectric devices.

### *C. Depolarization in $HfO_2$-based Ferroelectrics*

Compared to conventional perovskite ferroelectrics such as lead zirconate titanate (PZT) and barium titanate (BTO), hafnium oxide-based ferroelectrics are typically reported with a thickness and relative permittivity which is one order of magnitude lower ($d_{FE} \sim 10$ nm, $\varepsilon_{FE} \sim 30$). Since the depolarization field arising from imperfect screening (2) – (3) depends on the $d_{FE}/\varepsilon_{FE}$ ratio, perovskite and hafnia-based ferroelectrics should exhibit comparable depolarization scaling effects. However, the coercive field ($E_c$) is an order of magnitude higher in $HfO_2$ ferroelectrics than perovskites, which suggests that the ferroelectric can withstand a higher depolarization field. The finite screening length induced depolarization field in a typical hafnia-based ferroelectric ($\varepsilon_{FE} = 30$) is calculated as a function of thickness with three different remanent polarization values assuming TiN electrodes with a screening length of 0.83Å ($m^* = 2.3m_0$, $\varepsilon_m = 4$, $n_0 = 4 \times 10^{22}$ cm$^{-3}$) [19], [20] as shown in Fig. 3.

The coercive field of $Hf_xZr_{1-x}O_2$ is around 1 MV/cm and when the depolarization field exceeds $E_c$, the ferroelectric is expected to reach a lower equilibrium polarization as a result of

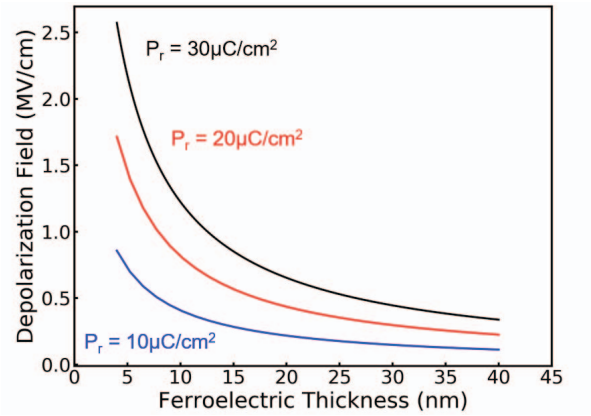


Figure 3. Depolarization field as a function of thickness in ferroelectric $Hf_xZr_{1-x}O_2$ calculated for a finite screening length with TiN electrodes.

transient polarization loss. Thus, very thin $Hf_xZr_{1-x}O_2$ films (< 5 nm) with a high $P_r$ (> 15 μC/cm$^2$) would likely stabilize at a lower remanent polarization as a result of depolarization. Therefore, ferroelectric tunnel junctions (FTJs) are expected to be challenging due to the mutual compromise which must be made between a large change in tunneling barrier height (made possible by the magnitude of switched polarization) and long term data retention (which requires a low depolarization field) [9].

In the case of the dielectric interfacial dead layer model, we directly compare PZT and $HfO_2$ assuming a range of values for the interfacial layer thickness and relative permittivity as shown in Fig. 4. It can be seen that in the worst cases for PZT and $HfO_2$ with a 1 nm interfacial dead layer and an interfacial relative permittivity of 14 and 50 respectively, the perovskite ferroelectric polarization state is predicted to become unstable around 50nm, where for $HfO_2$ it is 10 nm. Since the interfacial dead layer in $HfO_2$ is likely to be improved compared to PZT due to the more complex chemical composition of the perovskite, it is expected that ferroelectric polarization in $HfO_2$ could be stable below 5 nm and microscopic measurements have demonstrated ferroelectric switching at this scale [21]. Moreover, there has been some microscopic evidence that the dead layer in $HfO_2$ may consist of the tetragonal phase [22] which would strongly attenuate the strength of the depolarization at ultrathin thicknesses.

Due to the challenge of growing HZO films of different thicknesses with the same crystal phase fractions, studying the depolarization field by varying the ferroelectric thickness is difficult in polycrystalline hafnia ferroelectrics. Instead, we control the thickness of an $Al_2O_3$ dielectric inserted between the top ferroelectric metal interface to adjust the depolarization field. Because Si-based FeFETs require an interfacial layer between the ferroelectric and the Si channel, investigating the dielectric dead layer model in this way can give further insight into how such an interfacial layer can impact device reliability metrics such as cycling stability and data retention.

Final edited form was published in " 2019 19th Non-Volatile Memory Technology Symposium (NVMTS). Durham, 2019." ISBN 978-1-7281-4431-3
https://doi.org/10.1109/NVMTS47818.2019.9043368

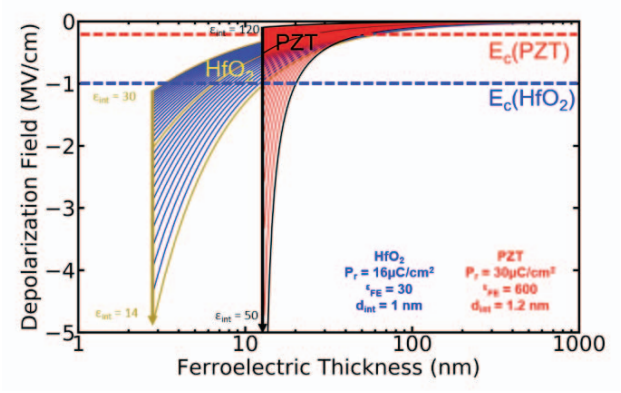


Figure 4. The thickness dependence of the depolarization field calculated for PZT and $HfO_2$-based ferroelectric for a range of different interfacial dead layer relative permittivity values.

## III. Fabrication and Experiment

Metal-ferroelectric-metal capacitors were fabricated on (100) Si wafers. 12 nm thick TiN bottom electrodes were sputtered at room temperature. Atomic layer deposition (ALD) was used to grow 8 nm thick $Hf_{0.5}Zr_{0.5}O_2$ thin films at 260 °C with an Oxford Instruments OpAl. TEMA-Hf and TEMA-Zr were used as the hafnia and zirconia precursors respectively and water was used as the oxidizer. $Al_2O_3$ was then deposited at the top HZO interface with thicknesses from 0.5 – 1.5 nm. 12 nm TiN top electrodes were then sputtered at room temperature. A post-metallization anneal of 600 °C for 20 s in $N_2$ was performed to crystallize the HZO films. Capacitor areas from 8000 $\mu m^2$ – 50,000 $\mu m^2$ were defined by evaporating Ti-Pt dots and using them as a hard mask in the subsequent step of wet etching the blanket TiN top electrode in SC1.

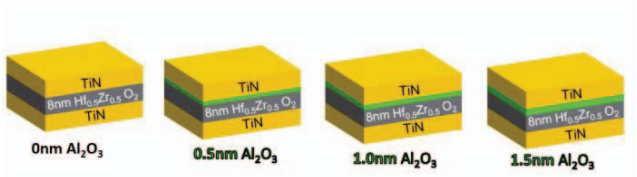


Figure 5. Fabricated devices with varying thicknesses of $Al_2O_3$ at the top TiN/HZO interface.

Ferroelectric polarization-voltage loops were taken on an Aixacct ferroelectric tester at 1 kHz with the bottom electrode grounded and the voltage applied to the top electrode. Wake-up cycling was performed at 10 kHz and ~3 MV/cm with bipolar square waves. Transient polarization measurements were performed with the Positive-Up-Negative-Down (PUND) waveform where the ramp time and pulse length was 100 μs long, and the delay between the pulses was varied from 1 μs – 10 s. Retention measurements were performed at room temperature and 85 °C with the same procedure as defined in a previous work [23].

## IV. Device Performance

### A. Wake-up

The extent to which the depolarization field suppresses the initial polarization, and how the polarization changes with electric field cycling, have not been clearly outlined. By directly inserting $Al_2O_3$ between the top electrode/ferroelectric interface, one can directly compare the differences in wake-up behavior between otherwise identical ferroelectric films. Hysteresis measurements in Fig. 6 show that the pristine or as-fabricated remanent polarization of the ferroelectric HZO films decreases with increasing $Al_2O_3$ interfacial layer thickness.

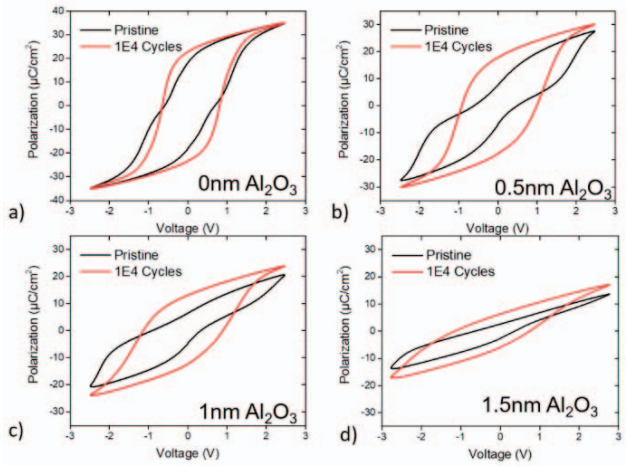


Figure 6. Polarization vs. voltage hysteresis curves before and after $10^4$ cycles with a) 0 nm, b) 0.5 nm, c) 1 nm, and d) 1.5 nm thick $Al_2O_3$.

The ferroelectric hysteresis loops look slightly pinched without any $Al_2O_3$ and become more antiferroelectric-like with the addition of 0.5 nm of $Al_2O_3$. Cycling the films opens up the hysteresis loop in all of the films and they lose the antiferroelectric-like shape seen in the pristine state. With a 1.5 nm thick $Al_2O_3$ layer, it is clear that ferroelectric switching is strongly suppressed as a result of the large voltage drop across the interfacial layer.

The increase in remanent polarization as a function of the number N of electric field cycles in the HZO film without any $Al_2O_3$ interfacial layer, as shown in Fig. 7a), can be well-described by

$$P_r = A\ln(N) + P_0 \qquad (10)$$

where A is the acceleration factor and $P_0$ is the initial remanent polarization. An extracted acceleration factor of 0.583 $\mu C/cm^2$ is in good agreement with other reports on wake-up [11], [12]. Interestingly, the $P_r$ dependence on the electric field cycle number deviates from (10) when an $Al_2O_3$ layer is inserted. Several slopes are clearly visible in these films which can be fitted by a piecewise application of (10) within certain cycling ranges. The normalized remanent polarization with wake-up cycling in Fig. 7 b) illustrates the much greater increase in $P_r$ with cycling with the introduction of the $Al_2O_3$ dead layer.

Final edited form was published in " 2019 19th Non-Volatile Memory Technology Symposium (NVMTS). Durham, 2019." ISBN 978-1-7281-4431-3
https://doi.org/10.1109/NVMTS47818.2019.9043368

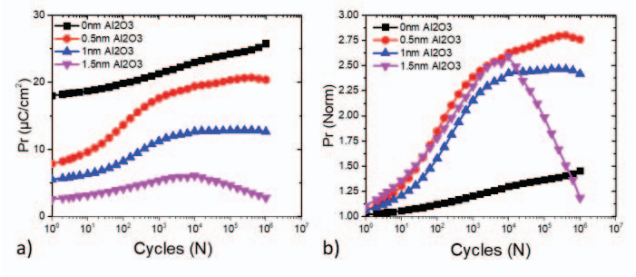


Figure 7. a) Remanent polarization as a function of electric field cycles. b) Normalized remanent polarization to the initial value as a function of electric field cycles.

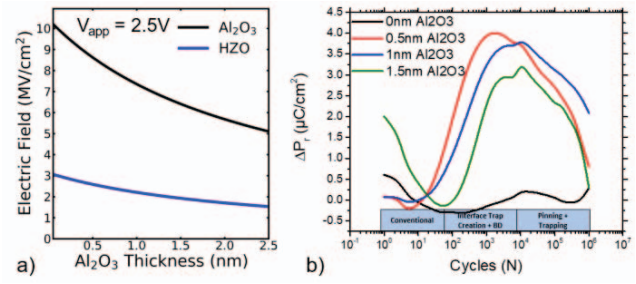


Figure 8. a) Magnitude of electric field across the $Al_2O_3$ and HZO layers with different $Al_2O_3$ interfacial layer thicknesses at an applied voltage of 2.5 V b) Change in remanent polarization with cycling when the conventional wake-up process is subtracted from the results in 7a).

During cycling, an applied voltage is creating an electric field across both the ferroelectric and interfacial layers. Fig. 8 shows how both the magnitude of the electric field and its change with varying $Al_2O_3$ thicknesses with the application of 2.5 V across the capacitor. As the $Al_2O_3$ layer is stressed for longer times by the > 5 MV/cm electric field during cycling, the layer will undergo breakdown [18] and trap states will be created at the interface. By subtracting the conventional wake-up process described by (10), it can be seen that the capacitors with an $Al_2O_3$ layer exhibit a sharp increase in remanent polarization between 50 – 1000 cycles which is subsequently followed by a strong decrease (Fig. 7b) in the rate of change of the remanent polarization.

The steep increase in $P_r$ ends after a higher number of electric field cycles when there is a thicker $Al_2O_3$ interface layer, suggesting that the number of cycles is cumulatively stressing the interface layer until time dependent dielectric breakdown events will have occurred throughout the layer. As the $Al_2O_3$ layer breaks down, a larger electric field will switch more ferroelectric charge and increase the remanent polarization. The decrease in $P_r$ after this gradual breakdown process implies that some portions of the HZO film are being suppressed by domain pinning. We predict that the $Al_2O_3$ layer effectively becomes a charge trapping layer after breakdown which enables greater charge carrier injection into the HZO layer where domains become unswitchable due to local Coulombic forces between trapped charge and individual dipoles. The degradation of the interfacial layer has been found to be the primary cause of the cycling limitations in FeFETs after $10^4$ cycles [25] which is in excellent agreement to the number of cycles observed in this work. In this approach evaluating the wake-up effect, field induced phase changes [26] can be excluded.

### *B. Transient Polarization Loss (t < 10 s)*

While the remanent polarization extracted from hysteresis gives an accurate depiction of the polarization at zero field during a dynamic measurement, it does not represent the usable polarization within an FeRAM memory cell because the time between read and write pulses can vary from µs to years. By introducing a thin $Al_2O_3$ interfacial layer at the FE/metal interface, the larger depolarization field is expected to lead to increased back-switching of ferroelectric domains. Thus, if the depolarization field is indeed strengthened, such back-switching would increase the amount of transient polarization defined as the switched polarization loss within 10 s of a write pulse.

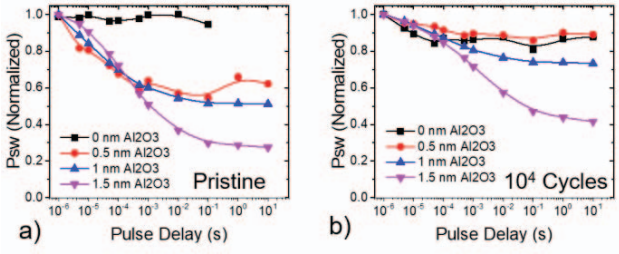


Figure 9. Normalized $P_{sw}$ with pulse delay time for a) pristine ferroelectric capacitors and b) after $10^4$ electric field cycles measured at room temperature.

The decrease in switched polarization at room temperature with delay time can be seen to get progressively worse with the thicker $Al_2O_3$ interfacial layers as seen in Fig. 9. In the as-fabricated HZO capacitors without an $Al_2O_3$ layer, there is virtually no polarization decay. The lack of observable polarization loss in this case originates from the rapid back-switching of domains which is observed already in these films as a pinched hysteresis loop. Thus, the pristine HZO capacitors have a smaller remanent polarization than the cycled capacitors even before 1 µs because back-switching is occurring dynamically when the pulse delay is smaller than 1 µs. In contrast, the cycled HZO capacitors undergo a decrease of roughly 10 % in $P_{sw}$ after 100 µs and then remain stable.

Unlike the HZO capacitors without an $Al_2O_3$ layer, cycling improves the transient polarization in capacitors with the interfacial $Al_2O_3$ layer inserted into the capacitor stack. For instance, in capacitors with a 0.5 nm $Al_2O_3$ layer, the polarization loss reduces from 55 % to 90 % after $10^4$ cycles. If the breakdown of the $Al_2O_3$ interfacial layer allows charge carriers to occupy trap states at the $Al_2O_3$/HZO interface, the closer proximity of these screening charges would consequently lower the depolarization field and improve the rapid polarization loss. Furthermore, this improvement with cycling diminishes as the $Al_2O_3$ thickness is increased which can be attributed to the decreased probability of carriers tunneling to occupy trap states at the $Al_2O_3$/HZO interface [27]. The depolarization field is calculated for each of the capacitors stacks as a function of HZO polarization in Fig. 10 and it can be seen that while the depolarization field is comparable between the finite screening

Final edited form was published in " 2019 19th Non-Volatile Memory Technology Symposium (NVMTS). Durham, 2019." ISBN 978-1-7281-4431-3
https://doi.org/10.1109/NVMTS47818.2019.9043368

case and with a 0.5 nm $Al_2O_3$ interfacial layer, the depolarization field doubles and then triples as the thickness of $Al_2O_3$ is increased from 1 to 1.5 nm. The enhanced strength of the depolarization field can thus explain severe, rapid polarization loss with thick interfacial layers.

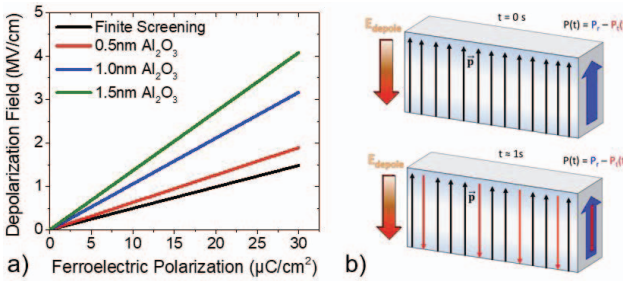


Figure 10. a) Depolarization field calculated in HZO capacitors as a function of polarization. b) Diagram illustrating the influence of the depolarization field and back-switching of ferroelectric domains with time.

### *C. Long Term Data Retention (t > 100 s)*

While the previous experiment has made it clear that there is rapid polarization loss with a stronger depolarization field, its effect on the long term polarization stability > 10 s has not been evaluated. Since long term data retention is a prerequisite for all non-volatile memory technologies, it is critical to understand to what extent depolarization can compromise ferroelectric memory devices. Retention measurements implicitly measure the loss of polarization in the Same-State (SS) and Next-Same-State (NSS) protocols, while the loss of switchable polarization through imprint is found in the Opposite State (OS) metric [23]. Both polarities for each retention metric are evaluated to account for differences in the stability of the two polarization states.

To achieve a baseline reference for all capacitors, retention measurements were taken at room temperature for all of the capacitor stacks (Fig. 11). It can be seen that there is virtually no decrease of the memory margins in HZO without an $Al_2O_3$ interfacial layer. A similar level of robustness is seen when only a 0.5 nm thick $Al_2O_3$ interfacial layer is present. However, the reduction in switched polarization lowers the overall memory margin with the incorporation of a 1 nm $Al_2O_3$ dielectric layer and there is some worsening of the OS margins with time suggesting that the imprint effect is more significant with the thicker interfacial layer. The memory window collapses entirely when a 1.5 nm thick $Al_2O_3$ layer is incorporated into the device stack. It can therefore be concluded that if the depolarization field is allowed to grow too large in strength, it can degrade an otherwise robust ferroelectric material with long term data retention.

Retention measurements were performed at 85 °C to more closely replicate application conditions and to accelerate the data retention loss in the ferroelectric capacitors. It was observed that the OS margins underwent the worst degradation due to imprint, while SS and NSS remained quite stable.

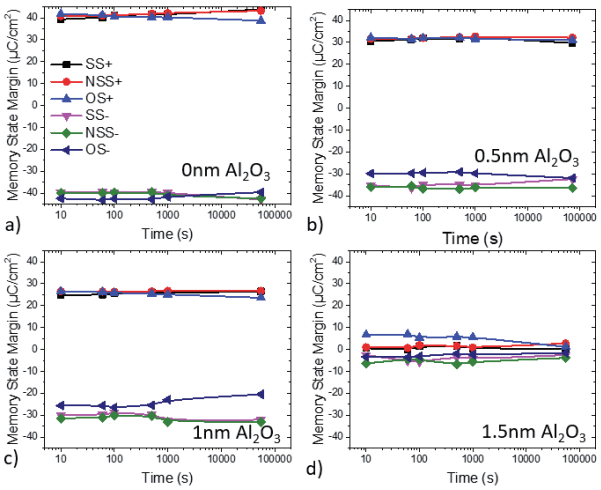


Figure 11. Retention measurements showing the memory state margins with read time taken at room temperature for HZO films with a) 0 nm $Al_2O_3$, b) 0.5nm $Al_2O_3$, c) 1nm $Al_2O_3$, and d) 1.5 nm $Al_2O_3$ at the top TiN/HZO interface. All of the capacitors underwent $10^4$ cycles before the measurement.

Due to the electric field across the interface caused by the ferroelectric polarization (9), charge carriers flow from the metal electrode to the $Al_2O_3$/HZO and increase the imprint effect during the elevated temperature bake. Using the OS margins as the worst case scenario for long term data retention in the ferroelectric capacitors, 10 year extrapolations showed that the capacitors with $Al_2O_3$ interfacial layers exhibited worse retention characteristics. Even the addition of 0.5 nm of $Al_2O_3$ caused a 28 % degradation in long term data retention compared to the HZO capacitor with no incorporated interfacial dielectric.

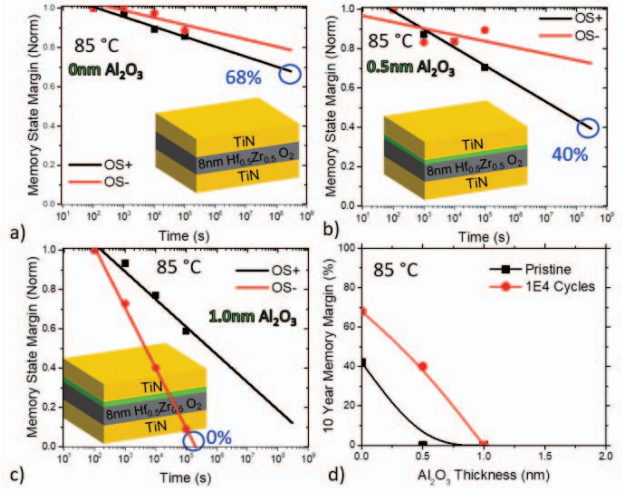


Figure 12. Retention measurements showing the memory margins with bake time taken at 85 °C for cycled HZO films with a) 0 nm $Al_2O_3$, b) 0.5nm $Al_2O_3$, c) 1nm $Al_2O_3$ extrapolated to 10 years (circled in blue). d) The extrapolated 10 year memory margins at 85 °C with $Al_2O_3$ thickness.

The HZO film without $Al_2O_3$ showed an above 40 % 10 year memory window retention at 85 °C in its as-fabricated

Final edited form was published in " 2019 19th Non-Volatile Memory Technology Symposium (NVMTS). Durham, 2019." ISBN 978-1-7281-4431-3
https://doi.org/10.1109/NVMTS47818.2019.9043368

state which improved to 68 % with cycling. This is a promising trend since long term data retention improvement with device use is beneficial, but further investigations are required to explore if this also stays true for larger numbers of cycles (> $10^9$). The capacitors investigated in this study must still exhibit significant differences when compared to the metal-ferroelectric-insulator-semiconductor (MFIS) gate stack of a FeFET, particularly with regard to trapping behavior and long-term retention since 10 year data retention has been shown for up to 150 °C with a 1.2 nm $SiO_2$ interfacial layer [28]. Efforts demonstrating improved retention and high temperature device operation with thicker ferroelectrics and higher k interfacial layers[29], [30], however, highlight the significant progress that can be made by designing the (MFIS) stack to diminish depolarization.

## V. Conclusion

Finite metal screening length and interfacial dead layer models were used to calculate the depolarization fields in $Hf_{0.5}Zr_{0.5}O_2$ with and without $Al_2O_3$ interfacial dielectric layers. The wake-up effect was significantly influenced by the introduction of the $Al_2O_3$ layer, with a strongly suppressed initial remanent polarization followed by a more rapid increase in $P_r$ from 50 – $10^4$ cycles in ferroelectric capacitors with the dielectric layer. The accelerated rate of wake-up with the capacitors with the $Al_2O_3$ layer was attributed to the gradual degradation and breakdown of the interfacial layer where the electric field exceeds 5 MV/cm during field cycling. After $10^4$ cycles, a decrease in the wake-up effect occurred in films with the incorporated dielectric layer. Since the degradation of the $Al_2O_3$ layer will facilitate a higher occupancy of trapped interface charge, it was predicted that such trapped carriers would migrate into the ferroelectric and pin domains.

Transient polarization measurements showed a strong dependency on the $Al_2O_3$ interfacial layer thickness which confirmed that back-switching of ferroelectric domains is strongly impacted by the depolarization field. HZO films with thicker $Al_2O_3$ layers showed rapid and severe polarization loss within 10 s, whereas comparable transient polarization characteristics were observed in the stack with no $Al_2O_3$ and 0.5 nm $Al_2O_3$ after wake-up. It was proposed that the improvement in transient polarization loss with cycling was due to the greater amount of trapped interface charge which brought screening charges into closer proximity with the ferroelectric, thereby reducing the depolarization field. A thick 1.5 nm $Al_2O_3$ layer completely collapses the ferroelectric memory window at room temperature, whereas the other ferroelectric capacitors exhibited robust retention. The projected 10 year data retention memory margins at 85 °C showed an improvement with wake-up cycling without $Al_2O_3$ and with the thinnest incorporated $Al_2O_3$ layer of 0.5 nm. The data retention was degraded with the incorporation of the dielectric interfacial layer and worsened with thicker layers at 85 °C. The success of emerging ferroelectric memories thus requires careful control of the ferroelectric thickness as well as any incorporated interfacial layers to minimize the impact of the depolarization field. Strategies to reduce depolarization in FeFETs and FTJs will be the key to export these emerging devices from the laboratory into semiconductor foundries.

## Acknowledgment

P.D.L is funded by the German Ministry of Economic Affairs and Energy (BMWi) project (16IPCEI310). M.H. received funding from the Electronic Component Systems for European Leadership Joint Undertaking under grant agreement no. 692519. This Joint Undertaking receives support from the European Union's Horizon 2020 research and innovation programme and Belgium, Germany, France, Netherlands, Poland and the UK. B.M received funding by the German Science Foundation (DFG).

## References

[1] J. Müller *et al.*, "Ferroelectricity in Simple Binary $ZrO_2$ and $HfO_2$," *Nano Letters*, vol. 12, no. 8, pp. 4318–4323, Aug. 2012.
[2] U. Schroeder, C. S. Hwang, and H. Funakubo, *Ferroelectricity in Doped Hafnium Oxide: Materials, Properties and Devices*. Woodhead Publishing, 2019.
[3] M. Pešić, S. Knebel, M. Hoffmann, C. Richter, T. Mikolajick, and U. Schroeder, "How to make DRAM non-volatile? Anti-ferroelectrics: A new paradigm for universal memories," in *2016 IEEE International Electron Devices Meeting (IEDM)*, 2016, pp. 11.6.1-11.6.4.
[4] T. Mikolajick, S. Slesazeck, M. H. Park, and U. Schroeder, "Ferroelectric hafnium oxide for ferroelectric random-access memories and ferroelectric field-effect transistors," *MRS Bull.*, vol. 43, no. 5, pp. 340–346, May 2018.
[5] B. Max, M. Hoffmann, S. Slesazeck, and T. Mikolajick, "Ferroelectric Tunnel Junctions based on Ferroelectric-Dielectric $Hf_{0.5}Zr_{0.5}O_2/Al_2O_3$ Capacitor Stacks," in *2018 48th European Solid-State Device Research Conference (ESSDERC)*, 2018, pp. 142–145.
[6] S. Dünkel *et al.*, "A FeFET based super-low-power ultra-fast embedded NVM technology for 22nm FDSOI and beyond," in *2017 IEEE International Electron Devices Meeting (IEDM)*, 2017, pp. 19.7.1-19.7.4.
[7] R. R. Mehta, B. D. Silverman, and J. T. Jacobs, "Depolarization fields in thin ferroelectric films," *Journal of Applied Physics*, vol. 44, no. 8, pp. 3379–3385, Aug. 1973.
[8] N. Gong and T. P. Ma, "Why Is FE–$HfO_2$ More Suitable Than PZT or SBT for Scaled Nonvolatile 1-T Memory Cell? A Retention Perspective," *IEEE Electron Device Letters*, vol. 37, no. 9, pp. 1123–1126, Sep. 2016.
[9] B. Max, M. Hoffmann, S. Slesazeck, and T. Mikolajick, "Retention Characteristics of $Hf_{0.5}Zr_{0.5}O_2$-Based Ferroelectric Tunnel Junctions," in *2019 IEEE 11th International Memory Workshop (IMW)*, 2019, pp. 1–4.
[10] M. Kohli, P. Muralt, and N. Setter, "Removal of 90° domain pinning in (100) $Pb(Zr_{0.15}Ti_{0.85})O_3$ thin films by pulsed operation," *Appl. Phys. Lett.*, vol. 72, no. 24, pp. 3217–3219, Jun. 1998.
[11] D. Zhou *et al.*, "Wake-up effects in Si-doped hafnium oxide ferroelectric thin films," *Applied Physics Letters*, vol. 103, no. 19, p. 192904, Nov. 2013.
[12] P. D. Lomenzo *et al.*, "TaN interface properties and electric field cycling effects on ferroelectric Si-doped $HfO_2$ thin films," *Journal of Applied Physics*, vol. 117, no. 13, p. 134105, Apr. 2015.
[13] S. Mueller *et al.*, "From MFM Capacitors Toward Ferroelectric Transistors: Endurance and Disturb Characteristics of $HfO_2$-Based FeFET Devices," *IEEE Transactions on Electron Devices*, vol. 60, no. 12, pp. 4199–4205, Dec. 2013.
[14] B. Max, M. Hoffmann, S. Slesazeck, and T. Mikolajick, "Direct Correlation of Ferroelectric Properties and Memory Characteristics in Ferroelectric Tunnel Junctions," *IEEE Journal of the Electron Devices Society*, pp. 1–7, 2019.
[15] M. Stengel and N. A. Spaldin, "Origin of the dielectric dead layer in nanoscale capacitors," *Nature*, vol. 443, no. 7112, pp. 679–682, Oct. 2006.
[16] L.-W. Chang, M. Alexe, J. F. Scott, and J. M. Gregg, "Settling the 'Dead Layer' Debate in Nanoscale Capacitors," *Advanced Materials*, vol. 21, no. 48, pp. 4911–4914, Dec. 2009.
[17] A. K. Tagantsev, I. Stolichnov, N. Setter, and J. S. Cross, "Nature of nonlinear imprint in ferroelectric films and long-term prediction of polarization loss in ferroelectric memories," *Journal of Applied Physics*, vol. 96, no. 11, pp. 6616–6623, Dec. 2004.
[18] P. Buragohain *et al.*, "Fluid Imprint and Inertial Switching in Ferroelectric La:$HfO_2$ Capacitors," *ACS Appl. Mater. Interfaces*, vol. 11, no. 38, pp. 35115–35121, Sep. 2019.

Final edited form was published in " 2019 19th Non-Volatile Memory Technology Symposium (NVMTS). Durham, 2019." ISBN 978-1-7281-4431-3
https://doi.org/10.1109/NVMTS47818.2019.9043368

[19] C. G. H. Walker, J. A. D. Matthew, C. A. Anderson, and N. M. D. Brown, "An estimate of the electron effective mass in titanium nitride using UPS and EELS," *Surface Science*, vol. 412–413, pp. 405–414, Sep. 1998.
[20] A. Schlegel, P. Wachter, J. J. Nickl, and H. Lingg, "Optical properties of TiN and ZrN," *J. Phys. C: Solid State Phys.*, vol. 10, no. 23, pp. 4889–4896, Dec. 1977.
[21] A. Chernikova *et al.*, "Ultrathin $Hf_{0.5}Zr_{0.5}O_2$ Ferroelectric Films on Si," *ACS Appl. Mater. Interfaces*, vol. 8, no. 11, pp. 7232–7237, Mar. 2016.
[22] E. D. Grimley *et al.*, "Structural Changes Underlying Field-Cycling Phenomena in Ferroelectric $HfO_2$ Thin Films," *Advanced Electronic Materials*, vol. 2, no. 9, p. 1600173, Sep. 2016.
[23] S. Mueller, J. Müller, U. Schroeder, and T. Mikolajick, "Reliability Characteristics of Ferroelectric Si:$HfO_2$ Thin Films for Memory Applications," *IEEE Transactions on Device and Materials Reliability*, vol. 13, no. 1, pp. 93–97, Mar. 2013.
[24] M. D. Groner, J. W. Elam, F. H. Fabreguette, and S. M. George, "Electrical characterization of thin $Al_2O_3$ films grown by atomic layer deposition on silicon and various metal substrates," *Thin Solid Films*, vol. 413, no. 1, pp. 186–197, Jun. 2002.
[25] E. Yurchuk *et al.*, "Charge-Trapping Phenomena in $HfO_2$-Based FeFET-Type Nonvolatile Memories," *IEEE Transactions on Electron Devices*, vol. 63, no. 9, pp. 3501–3507, Sep. 2016.
[26] M. Pešić *et al.*, "Physical Mechanisms behind the Field-Cycling Behavior of $HfO_2$-Based Ferroelectric Capacitors," *Advanced Functional Materials*, vol. 26, no. 25, pp. 4601–4612, 2016.
[27] M. Hoffmann, B. Max, T. Mittmann, U. Schroeder, S. Slesazeck, and T. Mikolajick, "Demonstration of High-speed Hysteresis-free Negative Capacitance in Ferroelectric $Hf_{0.5}Zr_{0.5}O_2$," in *2018 IEEE International Electron Devices Meeting (IEDM)*, 2018, pp. 31.6.1-31.6.4.
[28] E. Yurchuk *et al.*, "$HfO_2$-Based Ferroelectric Field-Effect Transistors with 260 nm Channel Length and Long Data Retention," in *2012 4th IEEE International Memory Workshop*, 2012, pp. 1–4.
[29] T. Ali *et al.*, "High Endurance Ferroelectric Hafnium Oxide-Based FeFET Memory Without Retention Penalty," *IEEE Transactions on Electron Devices*, vol. 65, no. 9, pp. 3769–3774, Sep. 2018.
[30] H. Mulaosmanovic, E. T. Breyer, T. Mikolajick, and S. Slesazeck, "Ferroelectric FETs With 20-nm-Thick $HfO_2$ Layer for Large Memory Window and High Performance," *IEEE Transactions on Electron Devices*, vol. 66, no. 9, pp. 3828–3833, Sep. 2019.